DAPNIA/SEA-99-08
CLIC Note 414

CLIC 3 TeV Interaction Region and Final Focus Studies

O. Napoly
CEA/Saclay, DAPNIA-SEA

August 16-28, 1999

Abstract

We discuss various design aspects of final focus system and interaction region (IR) for the 3 TeV version of the CLIC project, such as the choice of crossing angle, the effect of beamstrahlung, the possible impact of coherent pairs on the IR stability, and preliminary optics studies.

1 Introduction

In this note, we summarize various calculations dealing with the design of final focus system and the interaction region of the 3 TeV centre of mass energy version of the CLIC project. The CLIC 3 TeV parameters at the IP are recalled in Table 1.

Energy	E_0	GeV	1500
IP spot sizes	σ_x^* , σ_y^*	nm	40 , 0.6
Normalised emittances	$\gamma\epsilon_x$, $\gamma\epsilon_y$	μm	0.6 , 0.01
IP convergence	θ_x^* , θ_y^*	μrad	5.1 , 5.7
IP beta functions	β_x^* , β_y^*	mm	7.8 , 0.11
Bunch population	N_b	-	4×10^9
Bunch length	σ_z	μm	30
Repetition rate	f	Hz	75
Number of bunch per train	n_b	-	150
Bunch separation	τ_b / d_b	ns / m	0.67 / 0.2
Length of bunch train	T_{bt} / L_{bt}	ns / m	100 / 30
Beam power per side	P_B	MW	10.8
Average luminosity w/o pinch	$\mathcal{L}_0$	$\mathrm{cm}^{-2}\ \mathrm{s}^{-1}$	5.9×10^{34}

Table 1: CLIC 3 TeV parameters

2 The choice of the crossing angle

The loss of luminosity $\mathcal{L}$ due to finite crossing angle α, in the case of *rigid beams*, is given by the following expression :

$$\frac{d\mathcal{L}}{\mathcal{L}} = \frac{1}{\sqrt{1 + \left(\tan(\frac{\alpha}{2})\frac{\sigma_z}{\sigma_x^*}\right)^2}}.$$

It shows that the loss of luminosity can be expected to be large when the crossing angle is larger than the so-called 'diagonal angle' of the beam $\alpha_\Delta = \sigma_x^*/\sigma_z$. For the CLIC 3 TeV parameters of

Table 1, the diagonal angle is $\alpha_\Delta = 1.3$ mrad. In the presence of *beam-beam forces*, the loss of luminosity calculated from GUINEA-PIG[1] simulations is slightly larger, as shown in Fig.1.

One the other hand, a large enough crossing angle is necessary to avoid a multi-bunch kink instability to develop in the bunch train, due to the parasitic collisions away from the main interaction point (IP). There are 299 such parasitic collision points, separated by 10 cm, along the ± 15 m on both sides of the IP. To calculate this instability, a key ingredient is the intensity of the vertical beam-beam kick θ_y^* for vertical orbit differences δy^* at the IP. For small deviations, one can use a linear relation $\theta_y^* = \delta y^*/f_y$ where f_y is the focal distance of the *coherent* beam-beam interaction. For rigid beams, it is given by the disruption parameter

$$D_y = \frac{\sigma_z}{f_y/2} = \frac{2\, r_e\, N_b\, \sigma_z}{\gamma\, \sigma_y^*(\sigma_x^* + \sigma_y^*)} \approx 9.5$$

which leads to $f_y = 6.4\ \mu$m. With beam-beam forces, the linear beam-beam kick is weaker, as shown by the vertical beam-beam scan in Fig.2 (b). Accordingly, the focal length is bigger and, from Fig.2, we estimate it to be

$$f_y \approx \frac{2.4\,\text{nm}}{87\,\mu\text{rad}} = 28\,\mu\text{m}\,.$$

This value is used to estimate the beam-beam kick at the IP in the calculation of the multi-bunch luminosity as a function of the beam vertical jitter amplitude. For a crossing angle of 1.6 mrad, limiting the single-bunch luminosity loss to 20% , the instability seeded by the beam jitter is strong, as shown by Fig.3, even with 40 bunches and assuming that they don't interact beyond ± 2 m from the IP.

Clearly, the option of colliding at a small crossing angle, which was proposed for the 500 GeV c.m. energy CLIC parameters [3] is excluded for the 3 TeV parameters. This is essentially due to the fact that, although the energy is 6 times higher, the disruption parameter, and hence the beam-beam kick at the IP, has gone up from $D_y = 2$ for the 500 GeV parameters, to $D_y = 9.5$.

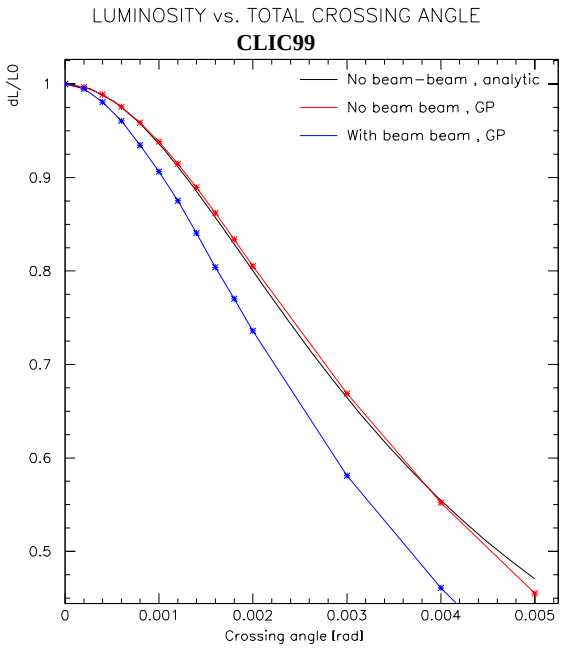

Figure 1: Luminosity loss as a function of the crossing angle α. The analytic expression is compared to Guinea-Pig simulation results with beam-beam forces off.

The only alternative is to collide with crab-crossing at a large angle : Fig.3 shows that the multi-bunch instability is totally suppressed already with a total crossing angle α =10 mrad. The calculation is done with 75 bunches per train and assuming that the bunches interact over $\pm$4 m on both sides of the IP.

3 Beam-beam effects

The beam-beam effects have been calculated with GUINEA-PIG in Ref.[3] and they are summarised in Table 2. We want to discuss two features of the beam-beam collisions which are specific of the so-called "large Υ regime" where the beamstrahlung photon emission lies in the quantum regime of synchrotron radiation.

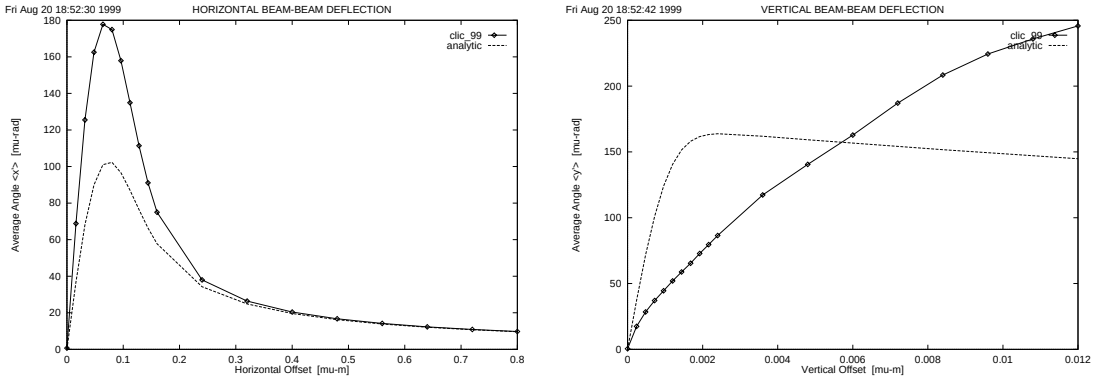

(a) Hor. beam-beam scan up to 20 σ_x^* offset.

(b) Vertical beam-beam scan up to 20 σ_y^* offset.

Figure 2: Beam-beam deflection simulations from GUINEA-PIG. The solid line shows the coherent deflection of rigid bunches (no coherent pairs).

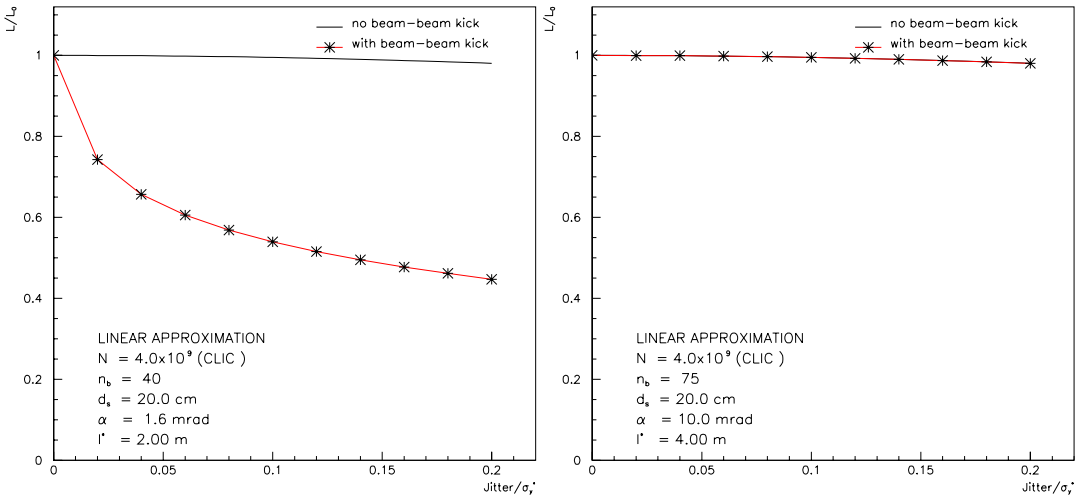

Figure 3: Multi-bunch luminosity as a function of the beam vertical jitter: α =1.6 mrad (left), α =10 mrad (right).

3.1 Vertical deflection at large offsets

Fig.2(b) reveals immediately that the vertical deflection of the beams at large vertical offsets operates in a quite different regime than in the lower energy designs, with $\Upsilon \ll 1$, where the deflection angle asymptotically tends to the rigid bunch curve describing far Coulomb interaction. The reason is that in the CLIC 3TeV case, the far Coulomb interaction is still in the quantum regime of synchrotron radiation. The 150 μrad deflection angle expected for 10 nm offset, for instance, corresponds to a bending field of 6250 T over a length given by $4\sigma_z = 120$ μm. The classical photon critical energy is then about 9 TeV and the corresponding average energy loss about 890 %. The correct handling of synchrotron radiation in the quantum regime leads to a roughly constant energy loss of about 32-38 % as shown by GUINEA-PIG simulations in Fig.4 (up,b). So the overshooting of the vertical beam-beam deflections at large offsets can be explained by the fact that the bunches lose a third of their energy on average during the collision.

Accordingly, the RMS energy spread of the beam ranges from 475 GeV to 495 GeV, and the vertical angular spread becomes very large for large vertical offsets[1] as shown in Fig.4 (down,b).

The consequences of the large energy loss and energy spread which is generated by beam-beam forces *even* when the beam miss each other by 10 to 20 sigmas at the IP in the vertical plane, must be carefully understood. Together with the large outgoing beam divergences, it will impact the beam extraction, making bending and focusing particularly challenging because of beam losses. It could also impact the IP tuning. For instance, cancelling the IP offset by the standard beam-beam kick diagnostics based on closeby BPMs will require large aperture and BPM dynamical range. Also, unless these BPMs are inboard of any magnet, the beam orbit measurements will be affected by strong energy dependence.

Notice finally that in the multi-bunch simulations of the preceding section, the smallest horizontal beam separation for the 1.6 mrad crossing-angle case at the first parasitic crossing is 160 μm which, according to Fig.2 (a) lies safely in the classical regime.

3.2 Impact of the coherent pairs on the IR stability

According to Ref.[3], about 8×10^8 pairs are produced, predominantly through the coherent process. Estimated from Figs. 2 and 3 of Ref.[3], the total energy carried by the pairs is roughly 40 Joules per bunch crossing (i.e. 6 kJ per bunch train) on each sides of the IP. This is six orders of magnitude larger than in the lower energy design like TESLA at 500 GeV centre of mass energy.

A possible consequence of this macroscopic energy is that the pairs might induce some vibrations of the material designed to dump their energy. Unless the 6 kJ per bunch train can be extracted away from the interaction region, these vibrations, naturally peaked at the dangerous 75 Hz beam frequency, might deteriorate the stability of the final doublet required for stabilizing the collisions.

Our argument is based on simplistic calculations which should be refined by more realistic

[1] These results should be carefully counter-examined by a better GUINEA-PIG expert since beam-beam simulations at large offsets require a large mesh which may not have been correctly optimized by the author. Also they might be quantitatively corrected once the coherent pairs are included in the simulation.

Average Luminosity	$\mathcal{L}$	$\mathrm{cm}^{-2}\ \mathrm{s}^{-1}$	1.3×10^{35}
Single bunch luminosity	$\mathcal{L}_{\mathrm{SB}}$	m^{-2}	1.1×10^{35}
Pinch factor	H_D	-	2.2
Average energy loss	δ_B	%	32
Average energy spread	σ_E	GeV	480
Number of e^+e^- pairs	N_P	-	8×10^8
Pair energy / bunch crossing / side	E_P	J	40
Averge power from pairs / side	P_P	kW	450

Table 2: Beam beam related parameters, as derived from GUINEA-PIG simulations.

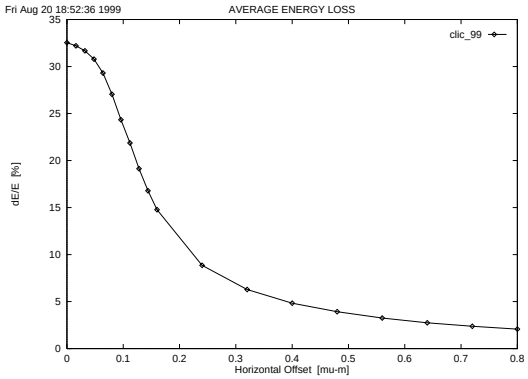

(a) Hor. beam beam deflections up to 20 σ_x^* offset.

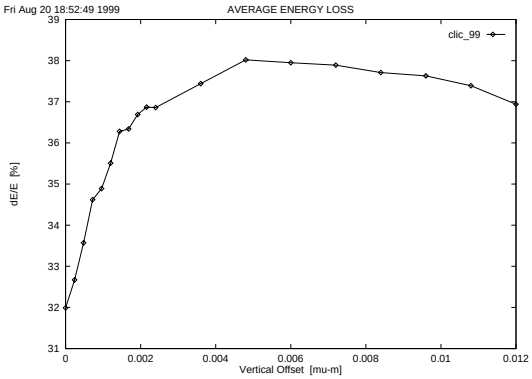

(b) Vertical beam-beam deflections up to 20 σ_y^* offset.

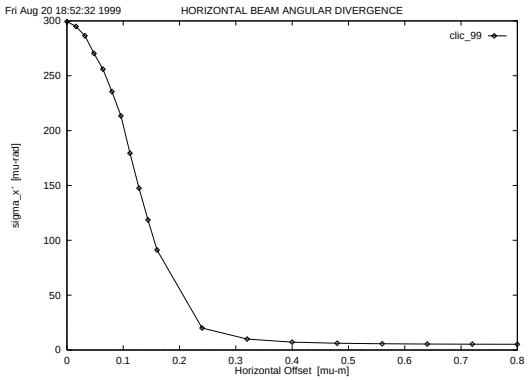

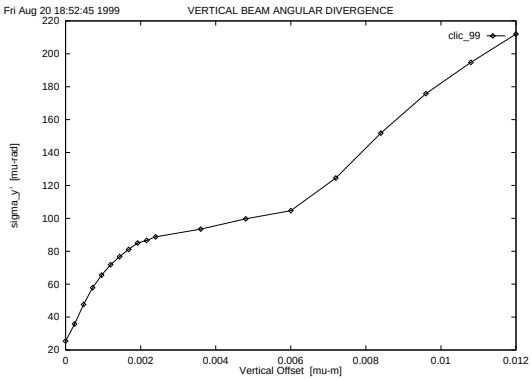

Figure 4: Average relative energy loss (up) and angular RMS divergence of the spent beams (down) for beam-beam deflection simulations with GUINEA_PIG (no coherent pairs).

mechanical and thermal calculations. We first consider the case where the pairs are dumped on a disk normal to their flux over a radius R and a length L. We assume that this volume contains all the showers and that the axial distribution of the pair particles is uniform.[2]The average temperature rise in the material for one bunch crossing, is given by

$$\Delta T = \frac{E_P}{L\,\pi R^2} \times \frac{1}{\rho} \times \frac{1}{c_h}$$

where ρ is the density and c_h the heat capacity of the material, ignoring all temperature dependence of these quantities. The expansion of the material in the direction of the pairs is given by

$$\delta L = \alpha\, L\, \Delta T = \frac{\alpha}{\rho c_h} \times \frac{E_P}{\pi R^2}$$

where α is the linear expansion coefficient. As shown in Table 3 for a few materials, Tungsten is the most favourable one to minimize the expansion. In convenient units, the expansion is given by

$$\delta L = 220 \text{ nm} \times \left(\frac{R}{1 \text{ cm}}\right)^{-2} \times n_b \text{ with } E_P = 40 \text{ J}$$

One bunch train, with $n_b = 150$, can therefore easily induce vibrations at the micrometer level. Of course some aperture is needed to clear the pairs.

Material	X_0 [cm]	ρ [g/cm^3]	c_h [J/gK]	α [10^{-6}/K]	$\rho c_h/\alpha$ [J/cm^3]
W	0.35	19.3	0.136	4.5	0.58×10^6
Fe	1.76	7.87	0.448	11.8	0.30×10^6
Cu	1.43	8.96	0.385	16.5	0.21×10^6
Ti	3.56	4.54	0.525	8.6	0.28×10^6
graphite	19.3	2.20	0.71	6.7	0.21×10^6

Table 3: Properties of some common materials.

We now consider a circular aperture of radius R at position L from the IP, and we assume that the pair particles propagate as in a drift space from the IP, neglecting the effect of the solenoid at these very high energies. We want to calculate the local expansion at the edge of this circular aperture. The integrated angular distribution of the pair energy flow can be roughly estimated from Fig.3 of Ref.[3], to be

$$\int_{\vartheta>\theta} \frac{dE}{d\vartheta} d\vartheta = E_T \times 10^{-5\theta/6\cdot10^{-3}}$$

since at 6 mrad the integrated distribution drops by five orders of magnitude. This gives for the angular distribution itself

$$\frac{dE}{d\theta} = \frac{5\,\ln 10}{6\cdot10^{-3}} \times E_T \times 10^{-5\theta/6\cdot10^{-3}}$$

from which the rms angle can be estimated to be

$$\sqrt{\langle\theta^2\rangle} \approx 0.74 \text{ mrad}$$

The local temperature rise at the edge of the aperture is then given by

$$\Delta T = \frac{dE_P}{L\,2\pi R\,dR} \times \frac{1}{\rho} \times \frac{1}{c_h} \text{ with } R = L\,\tan\theta \approx L\theta$$

The rest of the calculation goes like for the disk. One gets for the local expansion at the Tungsten edge after one bunch train :

$$\delta L(\theta) = 2.1\cdot10^{-8} \times \frac{1}{L^2\theta} \times 10^{-5\theta/6\cdot10^{-3}} \times n_b$$

[2]Usually, the pairs are more concentrated in the horizontal plane.

Requiring $\delta L < 1$ nm leads to $\theta > 6.8$ mrad for $L = 1$ m, or $\theta > 6.1$ mrad for $L = 2$ m.

The way the material expansion is going to affect the vertical sability of the doublet depends of course on the mechanical layout of the support systems. Ideally, a good symmetry with respect to the horizontal plane should guarantee a minimum vertical displacement. But on the other hand, the deposition of the pair particles will presumably be far from being axially symmetric, leading to local heatings and expansions much higher than calculated here.

Also, one could argue that what matters for tuning is not the amplitude of the vibrations once a steady regime is reached, but rather their fluctuations. Then, it is important to determine whether such a steady regime is stable or unstable against misteering of the beams. Incoherent pair production is very sensitive to luminosity variations, but in view of the results from Section3.1, the coherent pairs could be steadily produced even when the beams are misteered. This question requires more simulations and more work.

4 Optics of the final focus system

4.1 Last doublet

The last doublet properties are essentially fixed by the choice of l^*, the length from exit of the last quadrupole to the IP, and by the quadrupole gradient. Fig.5(a) shows the lengths of the F and D quadrupoles for $l^* = 2$ m and gradients ranging from 200 T/m to 600 T/m. Assuming a pole

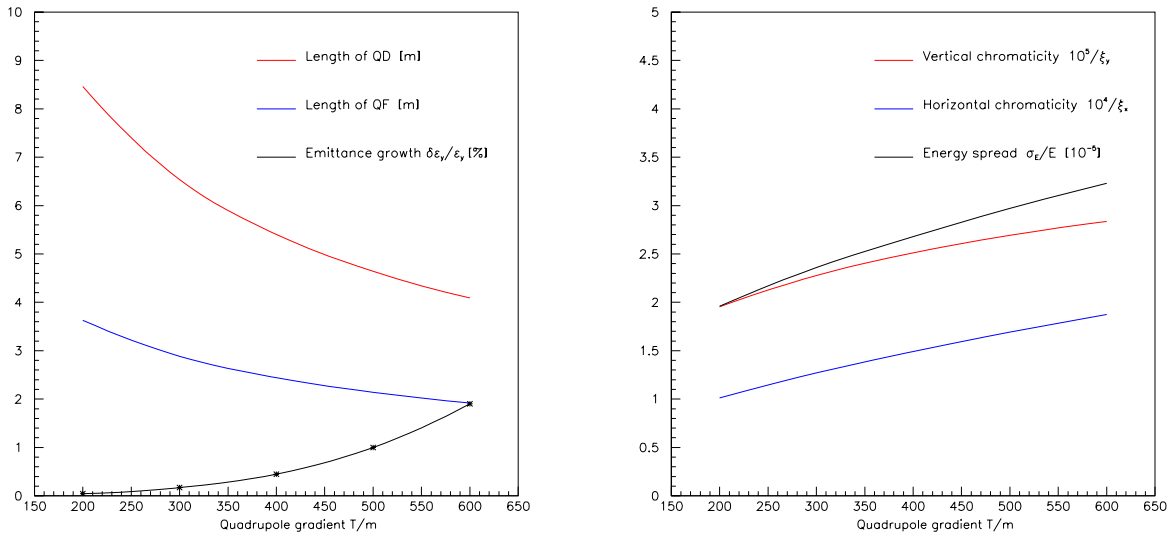

Figure 5: Doublet characteristics for 1.5 TeV beam energy and $l^* = 2$ m.

tip field of 1.5 T, the same figure shows the expected vertical emittance growth due to transverse resistive wakefields, assuming Cu resistivity, along the doublet aperture for a 1-sigma offset. We have assumed a 1 m long double inner drift space. This is not a very sensitive parameter, and shorter distances increase the countereffect and therefore the length of the individual quadrupoles. Fig.5(b) compares the inverse of the horizontal and vertical chromaticities $\xi_{x,y}$ to the RMS energy spread σ_δ induced by synchrotron radiation for a beam on axis in the doublet. It shows that the uncorrectable synchrotron energy spread is not small with respect to the vertical chromaticity, which is an indication that the Oide effect[4] from the doublet, is not negligible. Unfortunately, the product $\sigma_\delta \cdot \xi_{x,y}$, which should be smaller than 1, is almost independent of the quadrupole

gradient. It is known that the Oide effect is very insensitive to the doublet properties and can only be avoided by decreasing the vertical emittance of the beam (effectively, the vertical size of the beam in the quadrupole).

The result of tracking simulation through a doublet with 500 T/m, shown in Fig.6, confirms that the minimum spot size σ_y^* is about 1.0 nm for the current CLIC emittance. Synchrotron radiation will also be generated by defaults of straigthness of the quadrupole axis which, even static, cannot be corrected. As a first guess, the tolerance on this straightness should be smaller than the maximum beam size in the doublet, namely 21 μm.

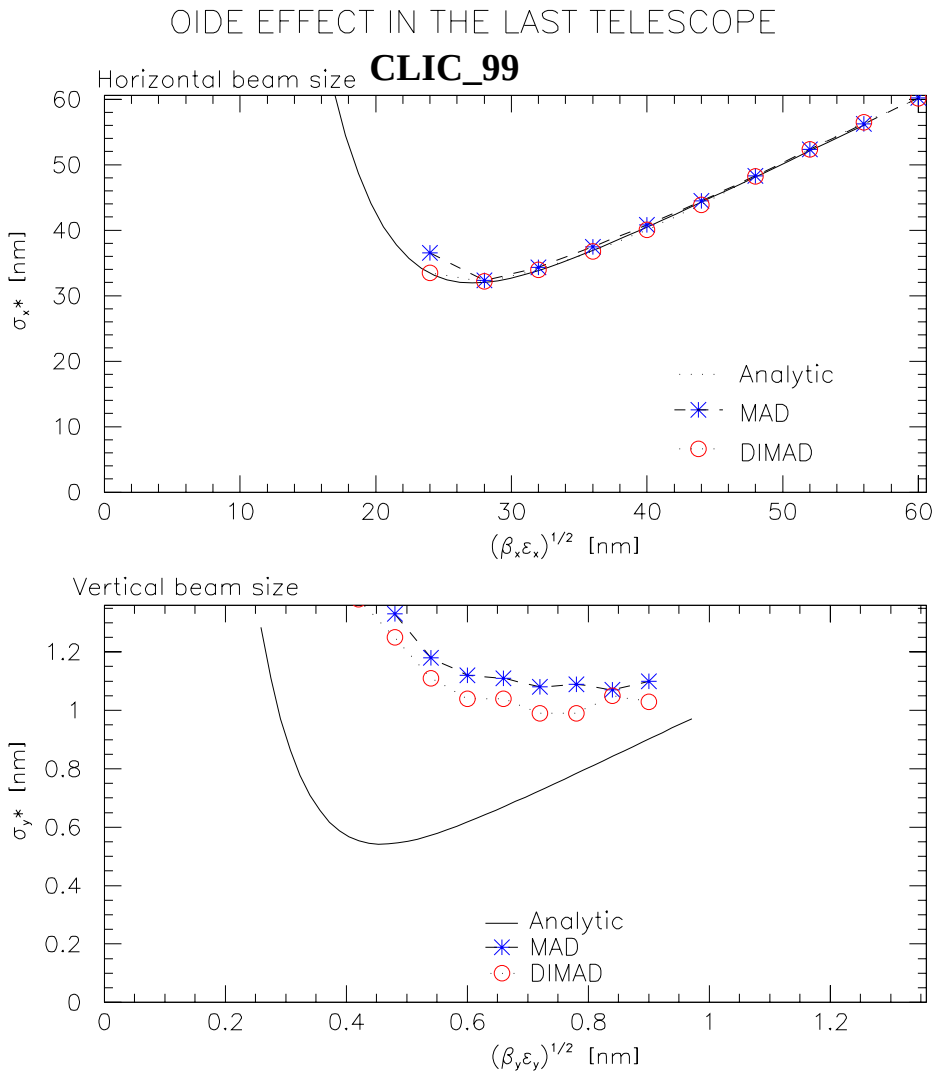

Figure 6: Spot size limitation due to synchrotron radiation in the last doublet.

4.2 Chromatic correction

With the large vertical chromaticity shown in Fig.5(b), chromatic correction is very difficult for quadrupole gradient below 500 T/m in the last doublet. We have investigated the normal and the odd dispersion schemes for chromatic correction section (CCS) based on pairs of π-separated

sextupoles. For the first optics, shown in Fig.7(a), the dispersion D_x is created symmetrically by 4 dipoles in the horizontal section CCSH and in the vertical section CCSV. In this way the second order dispersion T_{166} generated by the sextupole pairs vanishes independently in CCSH and in CCSV, while the x and y chromaticities are cancelled equally by the two sextupoles located at the two maxima of β_x (and D_x) in CCSH, and of β_y in CCSV. In the odd dispersion optics[5], shown in Fig.8(a), the sextupoles are at the same place but only 2 dipoles are necessary to create the dispersion in each section. The second order dispersion is then cancelled by a proper matching of the CCSH and CCSV dipoles. This matching imposes that the dipoles have the same sign, while in the "normal" dispersion scheme, the two families of dipoles can be tuned independently.

As can be seen from Figs.7(b) and 8(b), both designs lead to about the same bandwidth, which is insufficient for the expected energy spread from the linac. This is exhibited by the results of tracking simulations, including synchrotron radiation effects, for the "normal dispersion" scheme shown in Fig.9. Finding an optics with a suitable energy acceptance is certainly possible but requires more design work.

Acknowledgements

I would like to thank F. Ruggiero and F. Zimmermann for invitating me in the SL/AP group. I am grateful to F. Zimmermann for decisive help in the "odd dispersion" optics.

References

[1] D. Schulte, PhD Thesis, TESLA-97-08 (1996)

[2] O. Napoly, "Design of a Final Focus System for CLIC in the Multi Bunch Regime", CEA/DAPNIA/SEA-97-17, CLIC Note 351.

[3] D. Schulte, "High Energy Beam-Beam Effect in CLIC", CERN/PS 99-017, CLIC Note 391.

[4] K. Oide, Phys. Rev. Lett. 61, 1713 (1988); K. Hirata, K. Oide and B. Zotter, Phys. Lett. B224, 437 (1989).

[5] }K. Oide, "Final focus system with odd dispersion scheme" HEACC92, Hamburg, p. 2993 (1992).

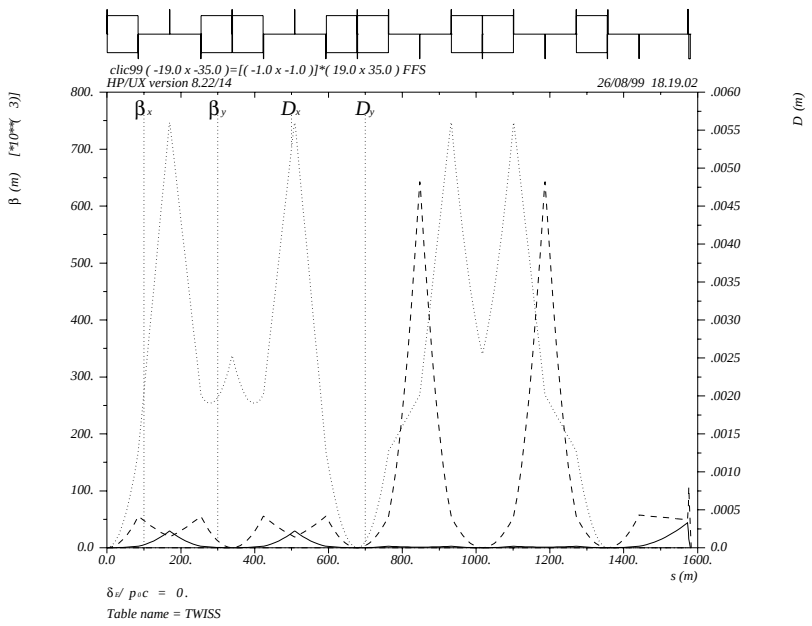

(a) Twiss functions and horizontal dispersion

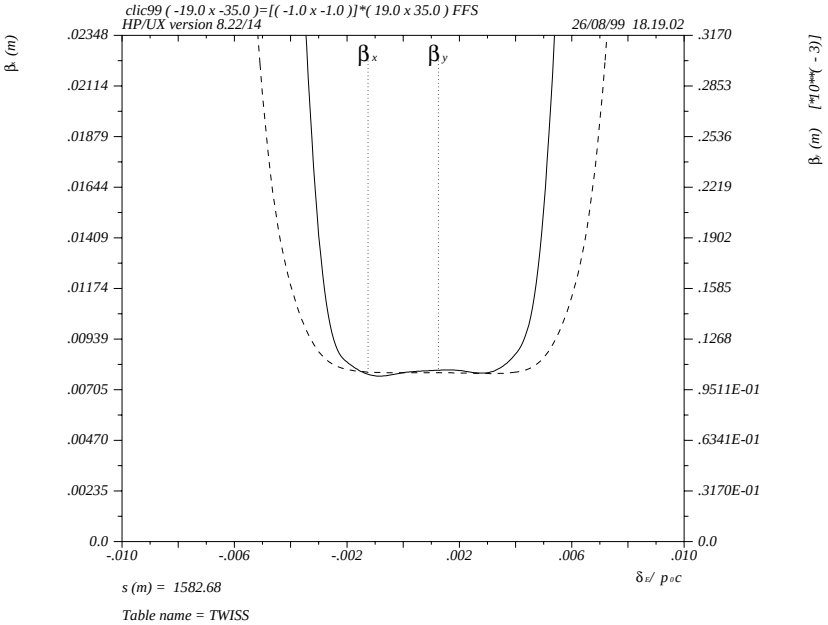

(b) Bandwidths

Figure 7: "Normal dispersion" optics.

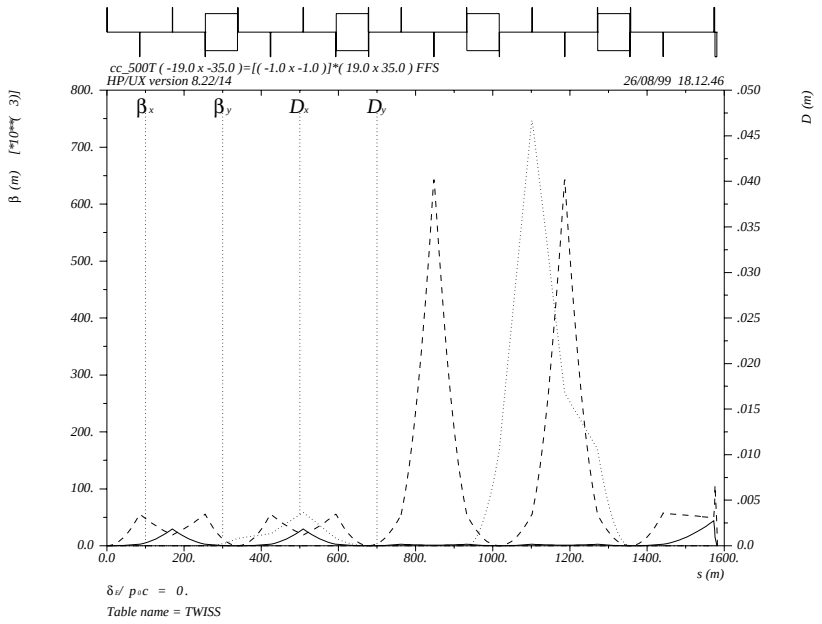

(a) Twiss functions and horizontal dispersion

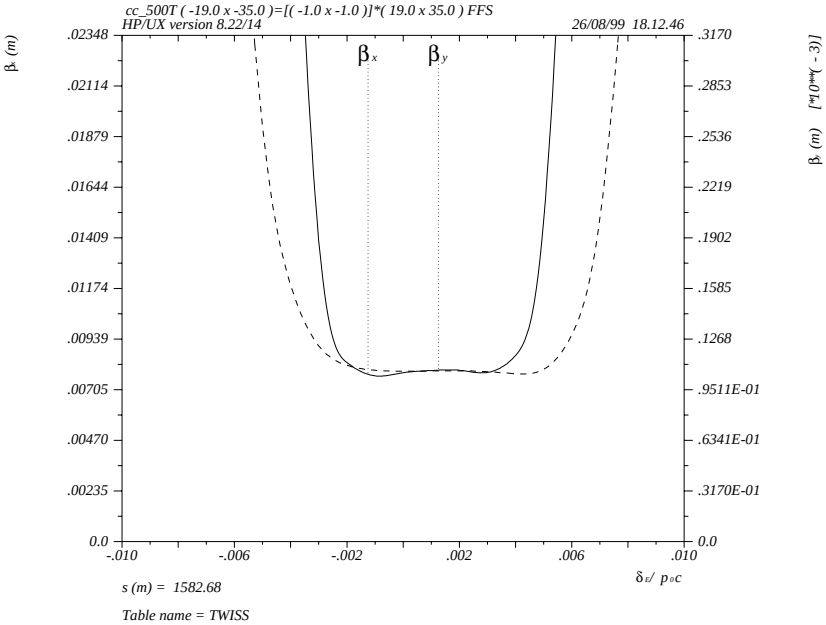

(b) Bandwidths

Figure 8: "Odd dispersion" optics.

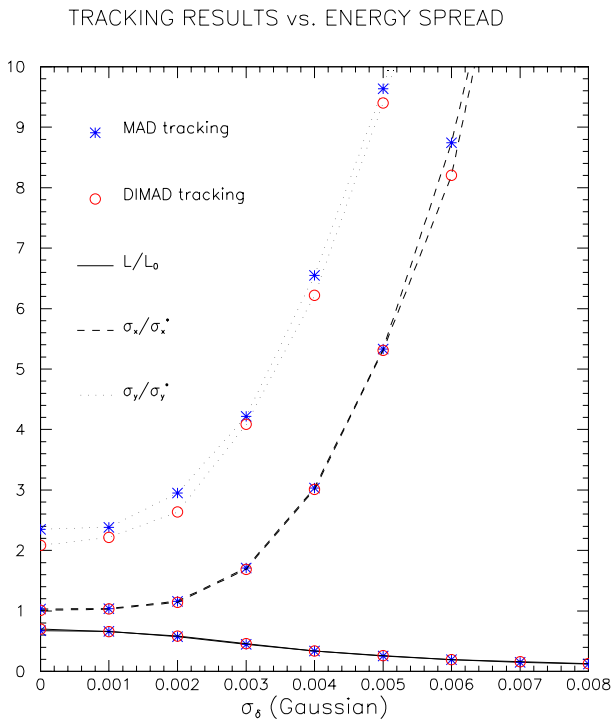

Figure 9: Tracking simulations for the "normal dispersion" FFS optics. The luminosity does not include beam-beam effects.